The Butyrate-Producing Bacterium *Clostridium butyricum* Suppresses *Clostridioides difficile* Infection via Neutrophil- and Antimicrobial Cytokine–Dependent but GPR43/109a-Independent Mechanisms

Atsushi Hayashi,*,† Hiroko Nagao-Kitamoto,* Sho Kitamoto,* Chang H. Kim,‡,§ and Nobuhiko Kamada*

Short-chain fatty acids, such as butyrate, are major gut microbial metabolites that are beneficial for gastrointestinal health. *Clostridium butyricum* MIYAIRI588 (CBM588) is a bacterium that produces a robust amount of butyrate and therefore has been used as a live biotherapeutic probiotic in clinical settings. *Clostridioides difficile* causes life-threatening diarrhea and colitis. The gut resident microbiota plays a critical role in the prevention of *C. difficile* infection (CDI), as the disruption of the healthy microbiota by antibiotics greatly increases the risk for CDI. We report that CBM588 treatment in mice significantly improved clinical symptoms associated with CDI and increased the number of neutrophils and Th1 and Th17 cells in the colonic lamina propria in the early phase of CDI. The protective effect of CBM588 was abolished when neutrophils, IFN-γ, or IL-17A were depleted, suggesting that induction of the immune reactants is required to elicit the protective effect of the probiotic. The administration of tributyrin, which elevates the concentration of butyrate in the colon, also increased the number of neutrophils in the colonic lamina propria, indicating that butyrate is a potent booster of neutrophil activity during infection. However, GPR43 and GPR109a, two G protein–coupled receptors activated by butyrate, were dispensable for the protective effect of CBM588. These results indicate that CBM588 and butyrate suppress CDI, in part by boosting antimicrobial innate and cytokine-mediated immunity. *The Journal of Immunology*, **2021, 206: 1576–1585.**

The gut microbiota contributes to the regulation of the host immune system and homeostasis. Numerous studies have demonstrated that the gut microbiota is associated with many pathological conditions, such as inflammatory bowel disease (1, 2), obesity (3, 4), diabetes (5, 6), rheumatoid arthritis (7), multiple sclerosis (8), graft-versus-host disease (9, 10), and infections (11, 12). Short-chain fatty acids (SCFA), especially butyrate, acetate, and propionate, are major metabolites produced by fermentation of dietary fiber by the gut microbiota (13). Butyrate promotes the epithelial barrier function (14) and induces antimicrobial peptides, such as regenerating islet-derived protein 3 (Reg3)γ and β-defensins (15). Butyrate is known for its potent epigenetic regulatory activity as a histone deacetylase inhibitor (HDACi) (16). Also, butyrate suppresses inflammatory responses, in part, by inhibiting NF-κB (17). G protein–coupled receptors (GPR) 41, 43, and 109a have been identified as the SCFA-sensing receptors (18). GPR43, which is highly expressed in epithelial cells and certain types of immune cells, such as neutrophils, binds to SCFA, specifically to butyrate (15, 19). GPR43 triggering by SCFA induces neutrophil chemotaxis (19, 20). GPR43 deficiency leads to reduced acute inflammation, as evidenced by delayed epithelial cytokine and neutrophil responses in animal models of colitis (20, 21). In chronic inflammatory conditions, GPR43-deficient mice showed increased inflammatory responses, which is consistent with defective acute responses and microbial invasion (20, 22). Consistently, GPR43-deficient mice infected with *Citrobacter rodentium* were more susceptible to infection than wild-type (WT) mice (22).

Clostridioides difficile is a Gram-positive, spore-forming bacterium that causes life-threatening diarrhea and colitis. The use of antibiotics decreases the overall diversity of the gut microbiota (dysbiosis), resulting in *C. difficile* infection (CDI) through the aberrant proliferation of *C. difficile*. Fecal microbiota transplantation is known to be an effective treatment for CDI (23). However, the risk of serious adverse events, likely due to transmission of pathogenic organisms, has prompted the Food and Drug Administration to issue a safety alert regarding the use of fecal microbiota transplantation to treat patients with CDI. A recent

*Division of Gastroenterology and Hepatology, Department of Internal Medicine, University of Michigan, Ann Arbor, MI 48109; †Miyarisan Pharmaceutical, Central Research Institute, Saitama 331-0804, Japan; ‡Department of Pathology, University of Michigan, Ann Arbor, MI 48109; and §Mary H. Weiser Food Allergy Center, University of Michigan, Ann Arbor, MI 48109

ORCIDs: 0000-0003-4060-2383 (A.H.); 0000-0003-3597-6647 (S.K.).

Received for publication March 30, 2020. Accepted for publication January 14, 2021.

This work was supported in part by research grants from Miyarisan Pharmaceutical (to N.K.), National Institutes of Health, National Institute of Diabetes and Digestive Diseases Grants R01 DK108901 (to N.K.) and P30 DK034933 (to S.K. and N.K.), and the Crohn's & Colitis Foundation (to N.K. and H.N.-K.).

A.H. and N.K. conceived and designed the experiments. A.H. conducted most of the experiments, with assistance from S.K. and H.N.-K. C.H.K. offered constructive advice and discussion. A.H. and N.K. analyzed the data. A.H. and N.K. wrote the manuscript with contributions from all authors.

The 16S rRNA gene sequences reported in this article have been submitted to the DNA Data Bank of Japan (https://www.ddbj.nig.ac.jp) under accession number DRA010918.

Address correspondence and reprint requests to Dr. Nobuhiko Kamada, Division of Gastroenterology and Hepatology, Department of Internal Medicine, University of Michigan, 1150 W. Medical Center Drive, MSRB1 6520C, Ann Arbor 48109, MI. E-mail address: nkamada@umich.edu

Abbreviations used in this article: CBM588, *Clostridium butyricum* MIYAIRI588; CDI, *C. difficile* infection; CPZ, cefoperazone; dKO, double knockout; GPR, G protein–coupled receptor; ILC, innate lymphoid cell; LP, lamina propria; LPMC, lamina propria mononuclear cell; OTU, operational taxonomic unit; Reg3, regenerating islet-derived protein 3; SCFA, short-chain fatty acid; Treg, regulatory T; WT, wild-type.

report has demonstrated that butyrate produced by gut microbiota mitigates the pathogenicity of colitis induced by *C. difficile* (24). Although it has been proposed that butyrate-induced HIF-1α–mediated strengthening of tight junctions is a potential mechanism for the protective effect of butyrate, the data are not convincing because of the dominant effect of HIF-1α deficiency over butyrate on CDI.

Unlike the pathogenic bacterium *C. difficile*, *Clostridium butyricum* MIYAIRI588 (CBM588), which is used as a live biotherapeutic product (also referred to as a probiotic) in clinical settings, lacks *Clostridium* toxin genes (25). Indeed, CBM588 administration antagonizes enteric pathogens, including *C. difficile*, *Candida albicans*, enterotoxigenic *Escherichia coli*, *Salmonella* spp., *Vibrio* spp., *Helicobacter pylori*, and enterohemorrhagic *E. coli* (26–28). Also, CBM588 suppresses inflammatory responses (29, 30) and contributes to the prevention of infectious disease (31) and antibiotic-associated diarrhea (32).

Antibiotics decrease the levels of butyrate-producing bacteria in the colon, thereby resulting in the impairment of the epithelial barrier and increasing susceptibility to pathogens (33). Despite recent progress, the precise mechanisms by which butyrate and CBM588 regulate the susceptibility and immune responses to CDI remain unclear. In this study, we show that CBM588 ameliorates CDI in mice through the induction of neutrophils and Th1 cells in the intestine. Butyrate induces neutrophil recruitment during CDI. Notably, the protective effect and neutrophil recruitment induced by CBM588 are mediated by GPR43/109a–independent mechanisms. Our data suggest that CBM588 boosts host immunity through neutrophils and antimicrobial cytokines, thus preventing the inflammation and mortality caused by CDI.

Materials and Methods

Animals

C57BL/6 WT mice were purchased from The Jackson Laboratory and housed and bred in the animal facility at the University of Michigan. GPR43$^{-/-}$109a$^{-/-}$ mice were obtained from Dr. S. Offermanns (Max Planck Institute for Heart and Lung Research, Bad Nauheim, Germany) (34, 35). To minimize the confounders caused by microbial differences, we used the mixed bedding protocol to normalize the gut microbiota (36). In all experiments, the microbiota of mice was normalized by mixed bedding for 2 wk prior to the experiments. All animal studies were approved by the University of Michigan Institutional Animal Care and Use Committee and performed in accordance with institutional guidelines.

CDI in mice

C57BL/6 WT, GPR43$^{-/-}$109a$^{-/-}$ mice (8–13 wk of age, female and male) were pretreated with cefoperazone (CPZ) (0.5 mg/ml) (MP Biomedicals) in sterile drinking water for 8 d, followed by 2 d of regular drinking water. Mice were then infected with 1×10^3 spores of *C. difficile* strain VPI 10463 administered by oral gavage on day 0. Body weight and clinical symptoms were monitored for the duration of the experiment. To count *C. difficile* colonization, fecal pellets were homogenized in PBS, plated on taurocholate-cycloserine-cefoxitin-fructose agar plates, and incubated anaerobically for 24 h at 37°C, as previously described (37). To deplete neutrophils, mice were injected i.p. with anti–Ly-6G mAb clone 1A8 (Bio X Cell) or control rat IgG2a (400 μg/200 μl) 1 d before CDI and then every 24 h. To neutralize IFN-γ, mice were injected i.p. with anti–IFN-γ mAb clone XMG1.2 (Bio X Cell) or control IgG1 (500 μg/200 μl) 1 d before CDI and then every 24 h. To neutralize IL-17A, mice were injected i.p. with anti–IL-17A mAb clone 17F3 (Bio X Cell) or control IgG1 (500 μg/200 μl) 1 d before CDI and then every 24 h. For SCFA treatment, mice were given 3 g/kg tributyrin (Sigma-Aldrich) 2 d before CDI and then daily for 3 d.

Preparation of the CBM588 strain and oral administration to mice with CDI

CBM588 was obtained from Miyarisan Pharmaceutical. The biochemical characteristics of this probiotic strain have been described previously (38). CBM588 was grown on nutrient agar (Nissui Pharmaceutical) containing 0.5% (w/v) glucose and 0.3% (w/v) $CaCO_3$ (Kanto Chemical) for 48 h in an anaerobic chamber. Colonies grown on the agar surface were suspended in sterile water at 1×10^9 CFU/ml. Mice were treated with 1×10^8 CFU of CBM588 2 d before CDI and then daily for 3 d.

C. difficile *germination and growth studies in antibiotic-treated mouse cecal content*

As previously described (37), mouse cecal content (non-CPZ– and CPZ-treated) was diluted with PBS (1:2 ratio) in an anaerobic chamber. Heat-treated *C. difficile* spores (65°C for 20 min) were added to the PBS-diluted murine cecal content and cocultured with or without CBM588 spores. This was followed by anaerobic incubation at 37°C for 6 h to assess germination and outgrowth. After incubation, bacterial enumeration was done on the taurocholate-cycloserine-cefoxitin-fructose agar selective medium. The remaining cecal content was heated at 65°C for 20 min to kill any vegetative cells and followed by bacterial enumeration.

Tissue preparation and flow cytometry

Single-cell suspensions of intestinal lamina propria (LP) mononuclear cells (LPMC) were prepared as previously described (29). Briefly, the colon and cecum were removed and cut into small pieces. The dissected mucosa was incubated with HBSS containing 1 mM DTT (Sigma-Aldrich) and 5 mM EDTA (Quality Biological) for 30 min at 37°C to remove the epithelial layer. The pieces of intestine were washed and placed in a digestion solution containing 1.5% FBS, 1.0 mg/ml collagenase type 3 (Worthington Biochemical), and 0.1 mg/ml DNase (Worthington Biochemical) for 1 h at 37°C. Intestinal supernatants were washed, resuspended in 40% Percoll, and overlaid on a 75% Percoll fraction. Percoll gradient separation was performed by centrifugation at $700 \times g$ for 20 min at room temperature. LPMC were collected at the interphase, washed, and resuspended in FACS buffer or RPMI 1640 medium (Life Technologies, Thermo Fisher Scientific) containing 10% FBS (Life Technologies, Thermo Fisher Scientific) and 1% penicillin/streptomycin (Life Technologies, Thermo Fisher Scientific).

For intracellular cytokine staining, cells were stimulated for 4 h with 50 ng/ml PMA (Sigma-Aldrich) and 1 μg/ml ionomycin (Sigma-Aldrich) in the presence of 1 μg/ml BD GolgiStop (BD Biosciences) in an incubator at 37°C. For cell surface staining of various molecules, cells were preincubated with an FcγR-blocking mAb (CD16/32; 2.4G2; BD Biosciences) for 20 min, followed by incubation with specific mAb for 20 min on ice. After staining surface molecules, the cells were resuspended in a fixation/permeabilization solution (BD Biosciences), and intracellular staining was performed. Standard six-color flow cytometric analyses were performed on the BD FACSCelesta (BD Biosciences), and data were analyzed using FlowJo software (BD Biosciences). Background fluorescence was assessed by staining with isotype-matched control mAb. FITC-, PE-, PerCP-Cy5.5–, allophycocyanin-, PE-Cy7–, allophycocyanin-Cy7– or Alexa Fluor 647–conjugated mAb against CD4 (GK1.5), CD3 (145-2C11), CD11b (M1/70), CD11c (N418), CD45 (30-F11), Ly-6G (1A8–Ly-6G), Ly-6C (HK1.4), Foxp3 (FJK-16S), Tbet (eBio4B10), IFN-γ (XMG1.2), and IL-17A (eBio17B7) were from eBioscience (Thermo Fisher Scientific), and RORγt (Q31-378) was from BD Biosciences. For the immune cell analysis, we first removed dead cells and debris and gated on lymphocytes using forward scatter/side scatter. Live leukocytes were then gated as CD45-positive and 7-aminoactionomycin D–negative cells. For the neutrophil and monocyte analysis, we pregated on CD11b$^+$ cells and then gated on Ly-6G and Ly-6C. For the T cell analysis, we gated on CD3$^+$ CD4$^+$ T cells. For non–T cells, we gated on CD3$^-$ CD4$^-$ cells. For intracellular transcriptional factor and cytokine analysis, we did not use 7-aminoactinomycin D staining.

Meta 16S rRNA gene sequencing

Genomic DNA was extracted using a modified QIAGEN DNeasy Blood and Tissue Kit protocol (QIAGEN). The 16S rRNA gene sequencing was performed as previously described (39). PCR was performed using MightyAmp DNA Polymerase Ver.3 (Takara Bio) and the Illumina forward primer 5′-AATGATACGGCGACCACCGAGATCTACAC (adaptor sequence) plus barcode (eight bases) plus ACACTCTTTCCCTACACGACGCTCTTCCGATCT (sequence primer) plus CCTACGGGNGGCWGCAG-3′ (341F) and the Illumina reverse primer 5′-CAAGCAGAAGACGGCATACGAGAT (adaptor sequence) plus barcode (eight bases) plus GTGACTGGAGTTCAGACGTGTGCTCTTCCGATCT (sequence primer) plus GACTACHVGGGTATCTAATCC-3′ (805R) to the hypervariable V3–V4 region of the 16S rRNA gene. Amplicons generated from each sample were subsequently purified using SPRIselect (Beckman Coulter). The amount of DNA was quantified using a Quantus Fluorometer and the QuantiFluor ONE

dsDNA System (Promega). Mixed samples were prepared by pooling approximately equal amounts of each amplified DNA and sequenced using the MiSeq Reagent Kit v3 (600 cycle) and the MiSeq sequencer (Illumina), according to the manufacturer's instructions.

Sequence analysis pipeline

The 16S rRNA sequence data generated by the MiSeq sequencer (Illumina) were processed by the Quantitative Insights into Microbial Ecology open-source bioinformatics pipeline (QIIME 1.9.1) (40, 41) at Miyarisan Pharmaceutical. Sequences with an average quality value <20 were filtered out. Chimeric sequences were removed using USEARCH (42). Sequences were clustered into operational taxonomic units (OTU) based on 97% sequence similarity at the species level using UCLUST (42) against the Greengenes Database gg 13_8 (43). A representative sequence for each OTU was aligned with PyNAST (40). Bacterial taxonomy was assigned using UCLUST (42). Genomic DNA from 20 strain even mix genomic material (American Type Culture Collection) was used to evaluate the data analysis procedures. Diversity analyses were run using the QIIME core_diversity_analyses.py script. Microbiota diversity was measured by the Shannon index.

Quantitative real-time PCR

Quantitative real-time PCR analysis was performed using Radiant SYBR Green Lo-ROX qPCR kit (Alkali Scientific). The primer sets used in this study were as follows: *Reg3b* forward, 5′-CTCTCCTGCCTGATGCTCTT-3′ and reverse, 5′-GTAGGAGCCATAAGCCTGGG-3′; *Reg3g* forward, 5′-TCAGGTGCAAGGTGAAGTTG-3′ and reverse, 5′-GGCCACTGTTACCACTGCTTTAGGATTGTCAAAAGATGTC-3′; and *MUC2* forward, 5′-GCCAAGGAAGGTGTCTGCA-3′ and reverse, 5′-CCTTGCAGTCAAACTCAAAGTGCT-3′.

Statistical analysis

The results were expressed as the mean ± SEM. Statistical analyses were performed using GraphPad Prism version 7.0 (GraphPad Software). Groups of data were compared using one-way ANOVA followed by the Bonferroni post hoc test or the Mann–Whitney *U* test. Differences at $p < 0.05$ were considered to be statistically significant.

Results

Oral administration of CBM588 protects mice against CDI

Mice were pretreated with CPZ to disrupt the healthy microbiota and then infected with *C. difficile* strain VPI 10463 to induce CDI. CBM588 was administered on day 2 and day 1 prior to CDI and on days 0, 1, 2 after CDI (Fig. 1A). The CBM588 treatment significantly reduced body weight loss and animal mortality caused by CDI, compared with the untreated control group (Fig. 1B, 1C). The decrease in the number of *C. difficile* colonization in the feces was slight but significant in the CBM588-treated group on day 1 postinfection (Fig. 1D). CBM588 administration significantly increased the expression of antimicrobial peptides, such as Reg3β and -γ gene expression in the cecum, whereas Muc2 expression did not change (Fig. 1E). Next, to characterize the effect of gut microbiota composition on the CBM588 protective effect, fecal samples were collected and analyzed by sequencing the 16S rRNA. Bacterial richness (the number of observed OTU) and α diversity (Shannon index) were reduced after CPZ treatment in both groups (Fig. 1F). CBM588 treatment restored neither the diversity nor the richness of the gut microbiota (Fig. 1F). Principal coordinates analysis plots of weighted UniFrac distances revealed that the microbiota profile in CBM588-treated mice was distinct from control mice before the *C. difficile* challenge (Fig. 1G). However, the structure of the microbiota in CBM588-treated mice remained different from the healthy protective microbiota (i.e., before CPZ treatment), suggesting that the gut microbiota may not be associated with the preventive effect of CBM588 against CDI (Fig. 1F, 1H). Next, we examined whether CBM588 directly suppresses the proliferation of *C. difficile* in the gut. To this end, cecal contents were collected from mice with and without CPZ treatment. *C. difficile* spores were inoculated into the cecal contents and cultured ex vivo. As previously reported (37), *C. difficile* growth was observed in the cecal contents isolated from CPZ-treated mice but not in the cecal contents isolated from mice with intact gut microbiota (Fig. 1J). CBM588 did not suppress the vegetative *C. difficile* growth ex vivo (Fig. 1J). These results demonstrate that CBM588 does not directly inhibit the germination or growth of *C. difficile*, nor does it alter the gut microbial structure. Rather, CBM588 may affect host immunity, which in turn suppresses the growth of *C. difficile* and attenuates *C. difficile*–induced damage in the intestine.

Immunomodulatory role of CBM588 in CDI

CBM588 has been shown to possess immunoregulatory and anti-inflammatory properties (29, 30). To determine whether CBM588 modulates host immunity to combat *C. difficile*, we analyzed immune cell profiles in the colonic LP of mice with or without CBM588 treatment. In the early phase of CDI, the administration of CBM588 significantly increased the number of Ly-6G$^+$ Ly-6C$^+$ neutrophils and Ly-6G$^-$ Ly-6C$^+$ monocytes in the colonic LP (Fig. 2A, 2B). To further examine the involvement of observed immunological changes in CBM588-mediated protection against CDI, we blocked neutrophil recruitment. As expected, the depletion of neutrophils by an anti–Ly-6G mAb canceled the protective effect of CBM588 on CDI (Fig. 2C–E). The number of *C. difficile* in the feces was not affected by neutralization (Fig. 2F). Consistent with our previous report (30), CBM588 treatment significantly increased Foxp3$^+$ regulatory T (Treg) cells in mice before the *C. difficile* challenge (Fig. 3A, 3B). In contrast, CBM588 treatment did not alter the frequency of Foxp3$^+$ Treg cells in the colon during CDI (Fig. 3A, 3B). In contrast, CBM588 treatment significantly increased the frequency of Tbet$^+$ Th1 cells and induced a higher production of IFN-γ and IL-17A by CD4$^+$ T cells (Fig. 3A, 3B). Of note, neither IFN-γ nor IL-17A production by non–T cells, such as innate lymphoid cells (ILC), was promoted by CBM588 treatment (Fig. 3C, 3D). Similar to neutrophil depletion, the administration of an IFN-γ or IL-17A neutralizing mAb attenuated the protective effect of CBM588 without affecting *C. difficile* colonization (Fig. 3E–L). These results indicate that CBM588 suppresses CDI through the induction of neutrophils and Th1 and Th17 cells in the colonic LP.

Tributyrin treatment promotes recruitment of neutrophils in the colonic LP after CDI

The beneficial effects of the SCFA, especially butyrate, produced by the gut microbiome, are well documented. In this context, it has been reported that disruption of the gut microbiota by CPZ treatment results in the reduction of SCFA, including acetate, propionate, and butyrate, in the cecum (33). Given that CBM588 can produce a robust amount of butyrate, we speculated that butyrate produced by CBM588 may regulate host immune defense, thereby rendering the host protected against CDI. Hence, we next examined the effect of butyrate on immune modulation during CDI. To this end, mice were given tributyrin, which elevates the concentration of butyrate in the colon, and then challenged with *C. difficile*. As tributyrin has been shown to protect mice from CDI (24), we examined its effect on the immune cells that were regulated by CBM588 treatment. Similar to CBM588, tributyrin significantly promoted the recruitment of neutrophils in the colonic LP during CDI (Fig. 4A, 4B). Unlike CBM588, tributyrin did not alter the production of IFN-γ and IL-17A by T cells (Fig. 4C, 4D). These results suggest that, in addition to promoting neutrophil recruitment in a butyrate-dependent manner, CBM588 promotes the differentiation of Th1 and Th17 cells and

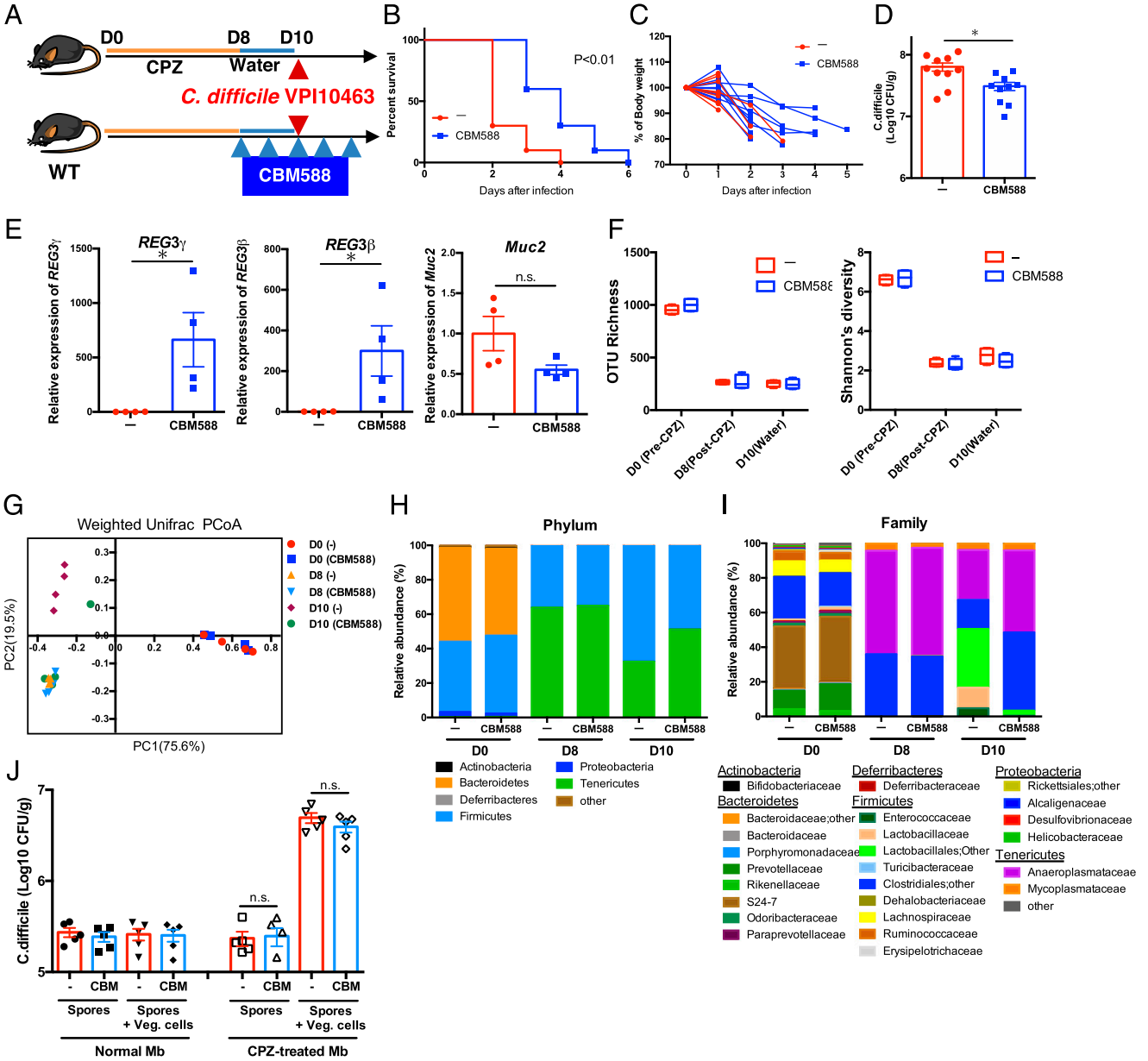

FIGURE 1. Oral administration of CBM588 protects the mice against CDI. (**A**) Experimental design included C57BL/6 WT mice that were pretreated with CPZ (0.5 g/l) in sterile drinking water for 8 d, followed by 2 d of regular drinking water. Mice were then infected with 1×10^3 spores of *C. difficile* VPI 10463. The mice were either untreated or orally inoculated with 1×10^8 spores of CBM588 after CPZ treatment. (**B**) Mice were assessed for survival after CDI. Survival curve is a combination of five independent experiments. (**C**) Change in body weight. (**D**) The number of *C. difficile* spores in feces on day 1 after CDI. (**E**) Expression of Reg3β and -γ and Muc2 mRNAs in the cecum, normalized to Actb expression. (**F**) Microbiota composition in feces was determined by 16S rRNA analysis. Differences in OTU and Shannon diversity indices at day 0 (pre-CPZ), day 8 (post-CPZ), and day 10 (before infection) between two groups. (**G**) The principal coordinates analysis plots show two groups of subjects defined by weighted UniFrac microbiota analysis on days 0, 8, and 10. (**H** and **I**) Taxon-based analysis at the phylum and family levels among the groups. Data are expressed as the percentage relative abundance. (**J**) Ex vivo growth of *C. difficile* in mouse cecal content with or without CPZ treatment. *C. difficile* and CBM588 spores in the cecal contents were cultured for 6 h to confirm the germination and outgrowth of *C. difficile*. Data are representative of two independent experiments, and statistical data are expressed as the mean ± SEM [(B–D) $n = 10$ per group, (C) $n = 4$ per group, (E–H) $n = 4$ per group, and (J) $n = 5$ per group]. $*p < 0.05$. Mb, microbiota; n.s., not significant.

their production of IFN-γ and IL-17A through a mechanism independent of butyrate production. Tributyrin administration caused a significant increase the expression of Reg3β and -γ genes in the colon (Fig. 4E), suggesting that butyrate induced the antimicrobial peptides. GPR43 is a known SCFA receptor, with an especially high affinity to butyrate (44). It has been reported that butyrate–GPR43 signaling is crucial for the recruitment of neutrophils (20). To this end, we used mice deficient in GPR43 and another receptor, GPR109a. Tributyrin treatment did not induce neutrophil recruitment by LPMC in GPR43/109a double knockout (dKO) mice with CDI (Fig. 4F, 4G), suggesting that tributyrin mediates GPR activation.

Protective effects of CBM588 in CDI are independent of GPR43/109a signaling

Hence, we next examined the importance of GPR43 in the protective effect of CBM588. GPR43/109a dKO mice were pretreated with CPZ and then challenged with *C. difficile* (Fig. 5A). CBM588 was administered before and after CDI, and the animal mortality and body weight were monitored. Contrary to our

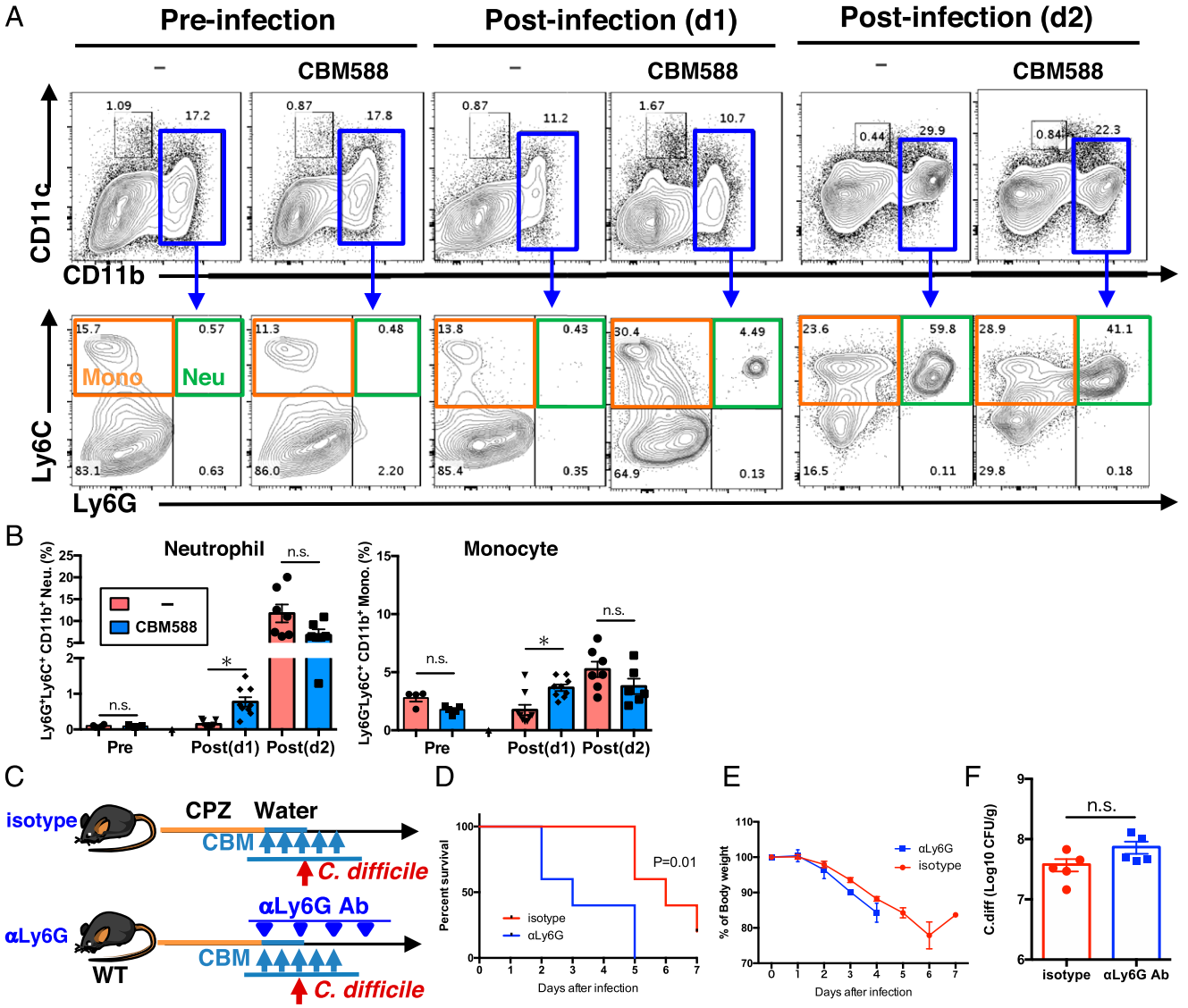

FIGURE 2. Protective effects of neutrophils induced by CBM588 treatment in the intestine after CDI. LPMC were isolated from WT mice before CDI and day 1 and day 2 after CDI. The mice were either untreated or orally inoculated with CBM588 after CPZ treatment. (**A**) Expression of Ly-6G$^+$ CD11b$^+$ neutrophils and Ly-6G$^-$ Ly-6C$^-$ CD11b$^+$ monocytes. (**B**) Statistical analysis of the percentages of neutrophils and monocytes. (**C**) C57BL/6 WT mice were pretreated with CPZ (0.5 g/l) in sterile drinking water for 8 d, followed by 2 d of regular drinking water. Mice were then infected with 1×10^3 spores of *C. difficile* VPI 10463. The mice were orally inoculated with 1×10^8 spores of CBM588 after CPZ treatment and then every 24 h. Neutralizing anti–Ly-6G mAb or control IgG (400 μg/200 μl) was administered 1 d before CDI and then every 24 h. (**D**) Mice were assessed for survival after CDI. (**E**) Change in body weight. (**F**) The number of *C. difficile* spores in feces on day 1 after CDI. Data are representative of two independent experiments, and statistical data are expressed as the mean ± SEM (n = 5–7 per group). *$p < 0.05$. Mono, monocyte; Neut, neutrophil; n.s., not significant.

expectation, the protective effect of CBM588 against CDI remained obvious in GPR43/109a dKO mice (Fig. 5B, 5C). Administration of CBM588 significantly reduced the number of *C. difficile* in these mice (Fig. 5D). As observed in WT mice, CBM588 treatment significantly increased recruitment of neutrophils during CDI (Fig. 5E, 5F). In contrast, unlike WT mice, CBM588 did not increase the number of Tbet$^+$ Th1 cells nor their production of INF-γ in GPR43/109a dKO mice (Fig. 5G, 5H). It has been reported that SCFA induce Reg3β and -γ in intestinal epithelial cells in WT but not GPR43$^{-/-}$ mice (15). Consistent with these observations, the administration of CBM588 did not increase Reg3β and -γ gene expression in GPR43/109a dKO mice (Fig. 5I).

Discussion

In the current study, we demonstrate that the butyrate-producing probiotic bacterium CBM588 prevents CDI through the recruitment of neutrophils and the activation of protective T cell immunity. The recruitment of neutrophils is likely elicited by butyrate produced by CBM588. Unexpectedly, the major butyrate receptors GPR43 and GPR109a were not required for the neutrophil recruitment induced by CBM588.

Neutrophils, also known as polymorphonuclear leukocytes, play various roles in the gastrointestinal tract, both beneficial and harmful (45). Neutrophils engulf and kill invading infectious agents and therefore mediate acute immune responses to clear pathogens, particularly bacterial and fungal pathogens (46). In contrast, excessive or sustained recruitment of neutrophils in the intestine can mediate chronic inflammatory responses such as occur in inflammatory bowel disease. Neutrophils not only elicit inflammation through the secretion of several inflammatory mediators (47), but they also promote the repair of damaged epithelial cell barriers (47). Consistent with this notion, the depletion

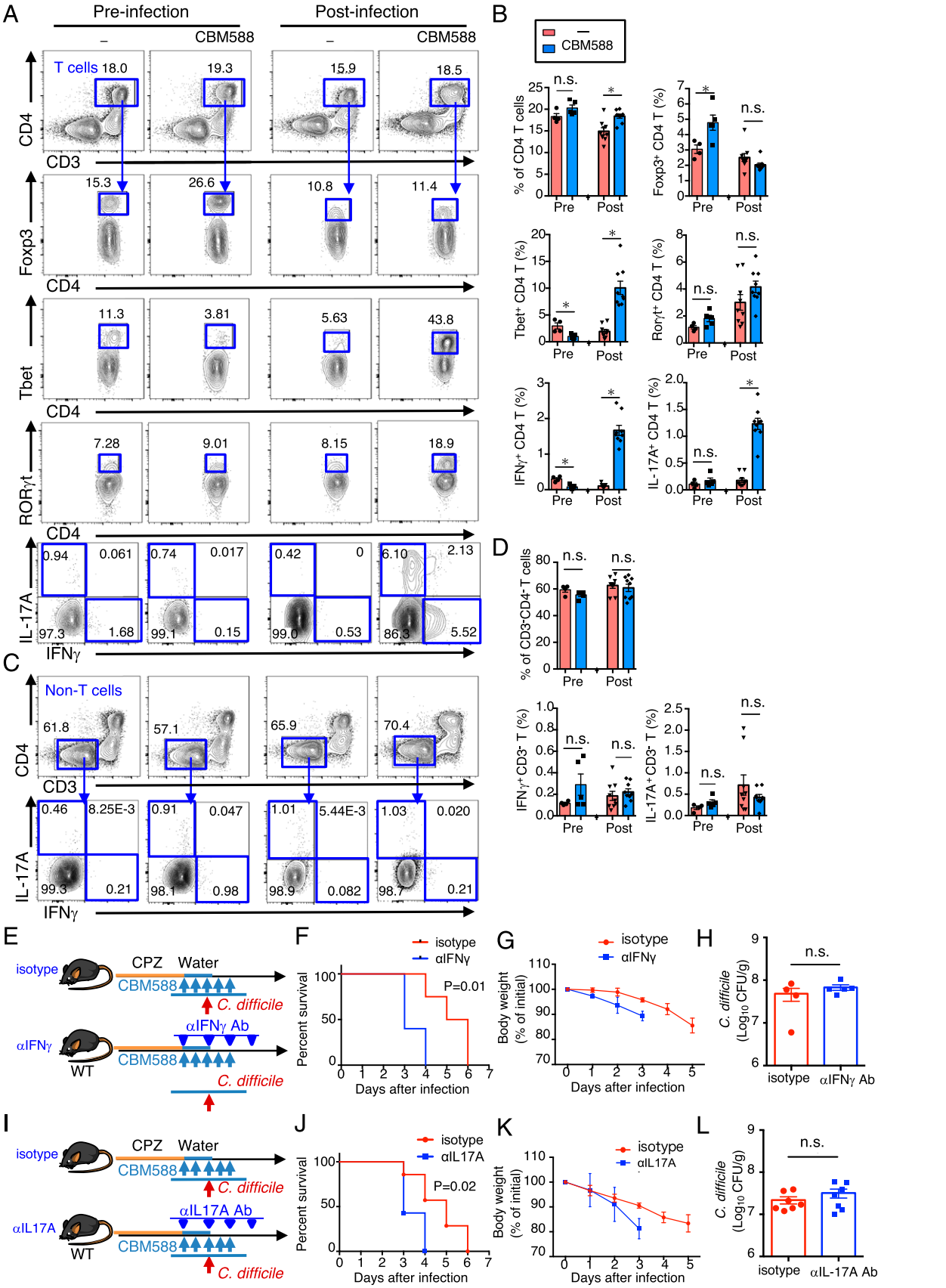

FIGURE 3. Protective effects of CBM588 in mice with CDI are IFN-γ and IL-17A dependent. LPMC were isolated from WT mice before CDI and day 1 after CDI. The mice were either untreated or orally inoculated with CBM588 after CPZ treatment. (**A**) Expression of $CD3^+$ $CD4^+$ T cells and Foxp3, Tbet, and RORγt within the $CD4^+$ cell populations. Frequency of IFN-γ^+ and IL-$17A^+$ CD4 T cells. (**B**) Statistical analyses of $Foxp3^+$, $Tbet^+$, RORγt$^+$, IFN-γ^+, and IL-$17A^+$ cells within the $CD4^+$ cell populations. (**C**) Expression of $CD3^-$ $CD4^-$ non–T cells and frequency of IFN-γ^+ and IL-$17A^+$ $CD3^-$ $CD4^-$ non–T cells. (**D**) Statistical analyses of IFN-γ^+ and IL-$17A^+$ cells within the $CD3^-$ $CD4^-$ non–T cell populations. (**E** and **I**) C57BL/6 WT mice were pretreated with CPZ (0.5 g/l) in sterile drinking water for 8 d, followed by 2 d of regular drinking water. Mice were then infected with *(Figure legend continues)*

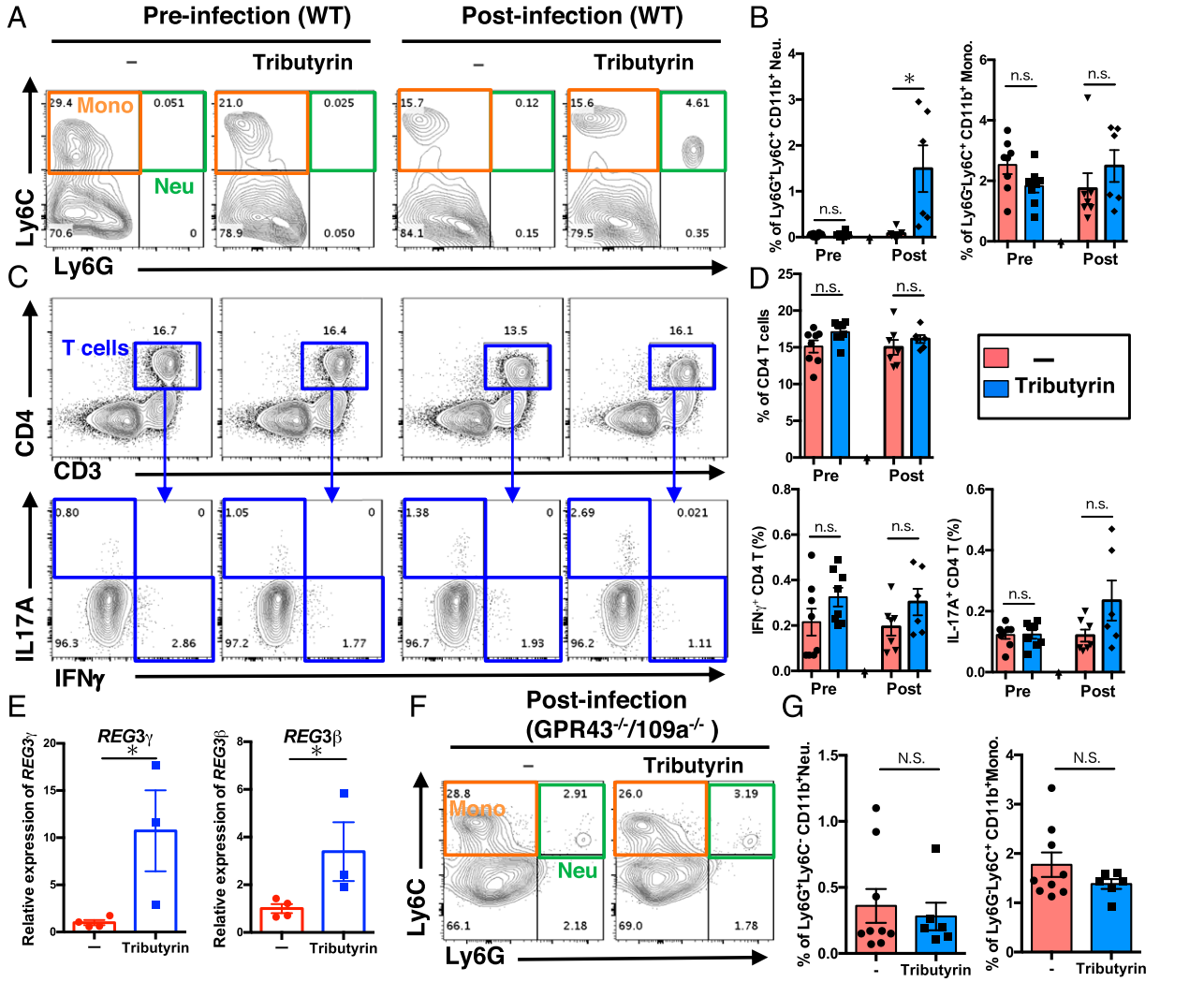

FIGURE 4. Butyrate treatment increases neutrophil recruitment in LPMC during CDI. Experimental design included C57BL/6 WT (**A**–**E**) or GPR43/109a dKO mice (**F** and **G**) that were pretreated with CPZ (0.5 g/l) in sterile drinking water for 8 d, followed by 2 d of regular drinking water. Mice were then infected with 1×10^3 spores of *C. difficile* VPI 10463. The mice were either untreated or orally administered 3 g/kg tributyrin twice per day after the CPZ treatment and then every 24 h. LPMC were isolated on day 1 postinfection, and the immune cell profile was analyzed. (A) Expression of Ly-6G$^+$ Ly-6C$^+$ CD11b$^+$ neutrophils and Ly-6G$^-$ Ly-6C$^+$ CD11b$^+$ monocytes in WT mice. (B) Statistical analysis of the percentages of neutrophils and monocytes. (C) Frequency of IFN-γ$^+$ and IL-17A$^+$ CD4 T cells. (D) Statistical analysis of the IFN-γ$^+$ and IL-17A$^+$cells within the CD4$^+$ cell populations. (E) Expression of Reg3β and -γ mRNAs in the cecum, normalized to Actb expression. (F) Abundance of Ly-6G$^+$ Ly-6C$^+$ CD11b$^+$ neutrophils (Neu) and Ly-6G$^-$ Ly-6C$^+$ CD11b$^+$ monocytes (Mono) in GPR43/109a dKO mice. (G) Statistical analysis of the percentages of neutrophils and monocytes. Data are representative of two independent experiments, and statistical data are expressed as the mean ± SEM [(A–D), (F), and (G) n = 6–8 per group and (E) n = 3–4 per group]. *$p < 0.05$. n.s., not significant.

of neutrophils impairs the regeneration of intestinal epithelial cells, thereby exacerbating mouse models of colitis (48). In this study, we observed that neutrophils seem to directly suppress the pathogen burden, as the colonization of *C. difficile* was significantly decreased in mice treated with CBM588. However, the depletion of neutrophils did not change the number of *C. difficile* in feces. In this regard, it is possible that neutrophils eradicate *C. difficile* that are associated with or that invade the mucosal tissue. In addition to a phagocytic role, neutrophils may contribute to the restoration of the epithelial barrier that is damaged by toxins produced by *C. difficile*. In all of these scenarios, neutrophil recruitment is likely a major host defense mechanism elicited by CBM588 against CDI. To our surprise, GPR43, which can function as a chemoattractant receptor triggered by SCFA gradients (49), is not required for CBM588-mediated neutrophil recruitment. In addition to the direct signaling effect through GPR43, SCFA may indirectly regulate neutrophils through the activation of other cell types, such as immune cells. In this regard, IL-17A promotes neutrophil recruitment and survival. The enhanced IL-17A production elicited by CBM588 may in part explain how

1×10^3 spores of *C. difficile* VPI 10463. The mice were orally inoculated with 1×10^8 spores of CBM588 after CPZ treatment and then every 24 h. Neutralizing anti–IFN-γ mAb, anti–IL-17A mAb, or control IgG (500 μg/200 μl) was administered 1 d before CDI and then every 24 h. (**F** and **J**) Mice were assessed for survival after CDI. (**G** and **K**) Change in body weight. (**H** and **L**) The number of *C. difficile* spores in feces on day 1 after CDI. Statistical data are expressed as the mean ± SEM (n = 4–9 per group). *$p < 0.05$. n.s., not significant.

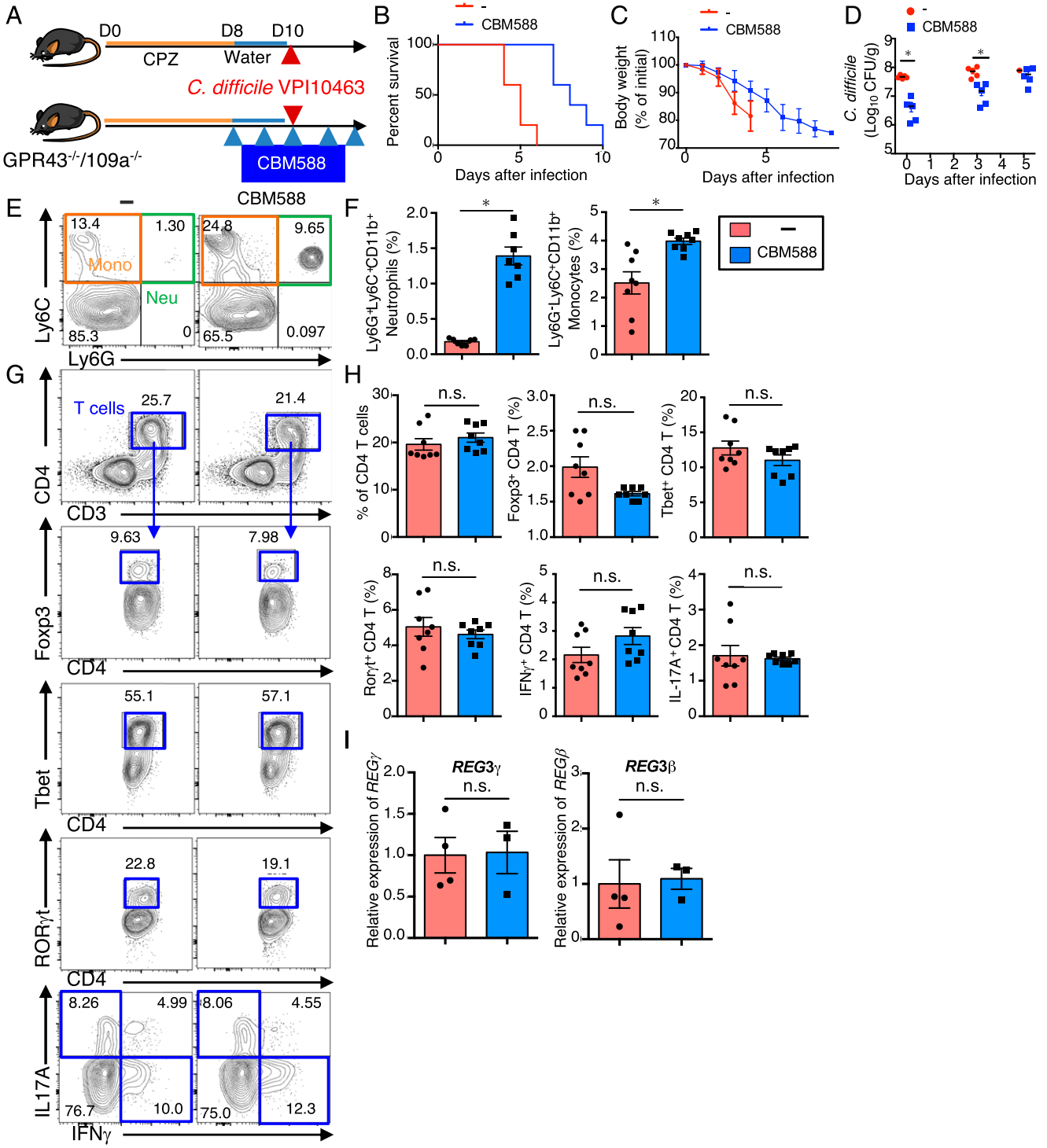

FIGURE 5. Protective effect of CBM588 in CDI is independent of butyrate–GPR43/109a pathways. (**A**) Experimental design included GPR43/109a dKO mice that were pretreated with CPZ (0.5 g/l) in sterile drinking water for 8 d, followed by 2 d of regular drinking water. Mice were then infected with 1×10^3 spores of *C. difficile* VPI 10463. The mice were either untreated or orally inoculated with 1×10^8 spores of CBM588 after CPZ treatment and then every 24 h. (**B**) Survival curve after CDI. (**C**) Change in body weight. (**D**) The number of *C. difficile* spores in feces at day 1 after CDI. (**E**) LPMC were isolated from GPR43/109a dKO mice after CDI. Abundance of Ly-6G$^+$ Ly-6C$^+$ CD11b$^+$ neutrophils (Neu) and Ly-6G$^-$ Ly-6C$^+$ CD11b$^+$ monocytes (Mono). (**F**) Statistical analysis of the percentages of neutrophils and monocytes. (**G**) Frequency of CD3$^+$ CD4$^+$ T cells, and Foxp3, Tbet, and RORγt within the CD4$^+$ cell populations. Frequency of IFN-γ$^+$ and IL-17A$^+$ CD4 T cells. (**H**) Statistical analyses of Foxp3$^+$, Tbet$^+$, RORγt$^+$, IFN-γ$^+$, and IL-17A$^+$ cells within the CD4$^+$ cell populations. (**I**) Expression of Reg3β and -γ mRNAs in the cecum, normalized to Actb expression. Data are representative of two independent experiments, and statistical data are expressed as the mean ± SEM [(B–D) $n = 5$ per group, (E–H) $n = 8$ per group, and (I) $n = 3$–4 per group]. *$p < 0.05$. n.s., not significant.

CBM588 potentiates the Th17 response independently of the butyrate–GPR43 pathway.

Another potential mechanism for the protective effect of CBM588 is the strengthening of barrier immunity by SCFA, as reported previously (50). Reg3β and -γ are antimicrobial peptides that protect the gut epithelial barrier from pathogenic bacteria (51). The CBM588 treatment significantly increased both Reg3β and -γ gene expression in the cecum of WT mice but not

GPR43/109a dKO mice. Thus, the induction of antimicrobial peptides by CBM588 is mediated by GPR43/109a. As the protective effect of CBM588 remained intact in GPR43/109a dKO mice, the induction of Reg3β and -γ by CBM588 may not have a major impact in the combat against *C. difficile*.

Although CBM588 has the potential to protect the host from CDI through the production of butyrate, CBM588 also harbors butyrate-independent anti–*C. difficile* mechanisms. We demonstrated that CBM588 administration significantly promotes the differentiation of IFN-γ–producing Th1 cells during CDI. Notably, this immune modulation was not elicited by tributyrin treatment, implying that it occurs independently of butyrate production. IFN-γ is known to have a protective function against *C. difficile*. Investigators have shown that IFN-γ, secreted by ILC1, can effectively control CDI (52). Consistently, we found that neutralization of IFN-γ secretion significantly attenuated the protective effect of CBM588. In the current study, most IFN-γ was produced by $CD4^+$ T cells (Th1 cells), not by ILC1. However, the induction of IFN-γ production was observed in the very early phase of infection (day 1 after CDI). This time frame may not allow the development of a *C. difficile*–specific Th1 response. Rather, IFN-γ production is likely an innate T cell response. Further studies are required to identify the detailed characteristics of IFN-γ–producing T cells in this model. Interestingly, CBM588 treatment failed to induce Th1 cells in GPR43/109a dKO mice. This is puzzling, as Th1 induction by CBM588 appeared to be butyrate independent. In this regard, it is reported that CBM588 produces not only butyrate but also other SCFA such as acetate and propionate (53). Hence, it is possible that propionate promotes Th1 differentiation through GPR43 activation. Moreover, it is also possible that non-SCFA products of CBM588 may increase the induction of Th1 cells.

Although CBM588 treatment resulted in the accumulation of neutrophils and Th1 cells during CDI, these changes were not observed in uninfected mice. Rather, CBM588 treatment induced anti-inflammatory–type immune responses, such as the generation of $Foxp3^+$ Treg cells. Thus, CBM588 can elicit both proinflammatory responses to fight pathogens and anti-inflammatory responses to maintain immune tolerance and homeostasis in the intestine. Although it remains unclear how CBM588 uses these opposing functions, it appears that they are regulated by host conditions. In this regard, it has been reported that SCFA promote a tolerogenic IL-10 response in the steady state but increase effector or inflammatory cytokine responses during *C. rodentium* infection (20, 54). Moreover, it has been also reported that bacteria can change their metabolic profiles, depending on their surrounding environment (e.g., inflammation) (55). Hence, it is possible that the production of metabolites, including but not limited to butyrate, by CBM588 is regulated by the host inflammatory environment and/or the interaction with other bacteria, such as *C. difficile*.

In this study, the broad composition of the gut microbiota seemed unaffected by CBM588. However, it is possible that CBM588 influences other commensal microbes that in turn suppress the colonization of *C. difficile*. In this context, it has been reported that the endogenous *C. difficile* strain LEM1 outcompetes highly pathogenic strains, such as the *C. difficile* strain VPI 10463 that was used in this study (56). Consequently, colonization by LEM1 attenuates disease caused by VPI 10463. Thus, it is possible that CBM588 influences the expansion of endogenous protective microbes in the gut in addition to eliciting protective host immunity, or perhaps, the expanded population of endogenous bacteria may elicit the host protective immunity. Further study would unravel the indirect protective effects that CBM588 achieves by modifying endogenous bacteria.

Collectively, these findings identify the role of the butyrate-producing bacterium CBM588 in boosting the activities of neutrophils and T cell immunity in the intestine to protect the host against CDI. It is noteworthy that significantly lower doses of CBM588 are used for human clinical trials as compared with animal models. Thus, in the clinical setting, treatment with CBM588 may fail to elicit host protective immunity. Nevertheless, this study elucidates the complexity of the host immune and microbial regulatory circuits and provides insight into the pathogenesis of acute CDI.

Acknowledgments

We thank Drs. Motomichi Takahashi, Kentaro Oka, Seiya Higashi, and Ayaka Minemura (Miyarisan Pharmaceutical) for technical assistance in the microbiome analysis and for contributing to constructive discussions, and we thank Dr. Stefan Offermanns (Max Planck Institute for Heart and Lung Research) for providing Gpr43/Gpr109a dKO mice.

Disclosures

A.H. is an employee of Miyarisan Pharmaceutical, N.K. received a research grant from Miyarisan Pharmaceutical. The other authors have no financial conflicts of interest.

References

1. Dalal, S. R., and E. B. Chang. 2014. The microbial basis of inflammatory bowel diseases. *J. Clin. Invest.* 124: 4190–4196.
2. Ni, J., G. D. Wu, L. Albenberg, and V. T. Tomov. 2017. Gut microbiota and IBD: causation or correlation? *Nat. Rev. Gastroenterol. Hepatol.* 14: 573–584.
3. Tilg, H., and A. Kaser. 2011. Gut microbiome, obesity, and metabolic dysfunction. *J. Clin. Invest.* 121: 2126–2132.
4. Schott, E. M., C. W. Farnsworth, A. Grier, J. A. Lillis, S. Soniwala, G. H. Dadourian, R. D. Bell, M. L. Doolittle, D. A. Villani, H. Awad, et al. 2018. Targeting the gut microbiome to treat the osteoarthritis of obesity. *JCI Insight* 3: e95997.
5. Cani, P. D., J. Amar, M. A. Iglesias, M. Poggi, C. Knauf, D. Bastelica, A. M. Neyrinck, F. Fava, K. M. Tuohy, C. Chabo, et al. 2007. Metabolic endotoxemia initiates obesity and insulin resistance. *Diabetes* 56: 1761–1772.
6. Paun, A., C. Yau, and J. S. Danska. 2017. The influence of the microbiome on type 1 diabetes. *J. Immunol.* 198: 590–595.
7. Zhang, X., D. Zhang, H. Jia, Q. Feng, D. Wang, D. Liang, X. Wu, J. Li, L. Tang, Y. Li, et al. 2015. The oral and gut microbiomes are perturbed in rheumatoid arthritis and partly normalized after treatment. *Nat. Med.* 21: 895–905.
8. Kadowaki, A., R. Saga, Y. Lin, W. Sato, and T. Yamamura. 2019. Gut microbiota-dependent CCR9+CD4+ T cells are altered in secondary progressive multiple sclerosis. *Brain* 142: 916–931.
9. Fredricks, D. N. 2019. The gut microbiota and graft-versus-host disease. *J. Clin. Invest.* 129: 1808–1817.
10. Fujiwara, H., M. D. Docampo, M. Riwes, D. Peltier, T. Toubai, I. Henig, S. J. Wu, S. Kim, A. Taylor, S. Brabbs, et al. 2018. Microbial metabolite sensor GPR43 controls severity of experimental GVHD. *Nat. Commun.* 9: 3674.
11. Fukuda, S., H. Toh, K. Hase, K. Oshima, Y. Nakanishi, K. Yoshimura, T. Tobe, J. M. Clarke, D. L. Topping, T. Suzuki, et al. 2011. Bifidobacteria can protect from enteropathogenic infection through production of acetate. *Nature* 469: 543–547.
12. Diep, B. A., S. R. Gill, R. F. Chang, T. H. Phan, J. H. Chen, M. G. Davidson, F. Lin, J. Lin, H. A. Carleton, E. F. Mongodin, et al. 2006. Complete genome sequence of USA300, an epidemic clone of community-acquired meticillin-resistant *Staphylococcus aureus. Lancet* 367: 731–739.
13. Koh, A., F. De Vadder, P. Kovatcheva-Datchary, and F. Bäckhed. 2016. From dietary fiber to host physiology: short-chain fatty acids as key bacterial metabolites. *Cell* 165: 1332–1345.
14. Zheng, L., C. J. Kelly, K. D. Battista, R. Schaefer, J. M. Lanis, E. E. Alexeev, R. X. Wang, J. C. Onyiah, D. J. Kominsky, and S. P. Colgan. 2017. Microbial-derived butyrate promotes epithelial barrier function through IL-10 receptor-dependent repression of claudin-2. *J. Immunol.* 199: 2976–2984.
15. Zhao, Y., F. Chen, W. Wu, M. Sun, A. J. Bilotta, S. Yao, Y. Xiao, X. Huang, T. D. Eaves-Pyles, G. Golovko, et al. 2018. GPR43 mediates microbiota metabolite SCFA regulation of antimicrobial peptide expression in intestinal epithelial cells via activation of mTOR and STAT3. *Mucosal Immunol.* 11: 752–762.
16. Flint, H. J., K. P. Scott, P. Louis, and S. H. Duncan. 2012. The role of the gut microbiota in nutrition and health. *Nat. Rev. Gastroenterol. Hepatol.* 9: 577–589.
17. Inan, M. S., R. J. Rasoulpour, L. Yin, A. K. Hubbard, D. W. Rosenberg, and C. Giardina. 2000. The luminal short-chain fatty acid butyrate modulates NF-kappaB activity in a human colonic epithelial cell line. *Gastroenterology* 118: 724–734.
18. Covington, D. K., C. A. Briscoe, A. J. Brown, and C. K. Jayawickreme. 2006. The G-protein-coupled receptor 40 family (GPR40-GPR43) and its role in nutrient sensing. *Biochem. Soc. Trans.* 34: 770–773.

19. Le Poul, E., C. Loison, S. Struyf, J. Y. Springael, V. Lannoy, M. E. Decobecq, S. Brezillon, V. Dupriez, G. Vassart, J. Van Damme, et al. 2003. Functional characterization of human receptors for short chain fatty acids and their role in polymorphonuclear cell activation. *J. Biol. Chem.* 278: 25481–25489.
20. Sina, C., O. Gavrilova, M. Förster, A. Till, S. Derer, F. Hildebrand, B. Raabe, A. Chalaris, J. Scheller, A. Rehmann, et al. 2009. G protein-coupled receptor 43 is essential for neutrophil recruitment during intestinal inflammation. *J. Immunol.* 183: 7514–7522.
21. Maslowski, K. M., A. T. Vieira, A. Ng, J. Kranich, F. Sierro, D. Yu, H. C. Schilter, M. S. Rolph, F. Mackay, D. Artis, et al. 2009. Regulation of inflammatory responses by gut microbiota and chemoattractant receptor GPR43. *Nature* 461: 1282–1286.
22. Kim, M. H., S. G. Kang, J. H. Park, M. Yanagisawa, and C. H. Kim. 2013. Short-chain fatty acids activate GPR41 and GPR43 on intestinal epithelial cells to promote inflammatory responses in mice. *Gastroenterology* 145: 396–406.e1–e10.
23. van Nood, E., A. Vrieze, M. Nieuwdorp, S. Fuentes, E. G. Zoetendal, W. M. de Vos, C. E. Visser, E. J. Kuijper, J. F. Bartelsman, J. G. Tijssen, et al. 2013. Duodenal infusion of donor feces for recurrent *Clostridium difficile*. *N. Engl. J. Med.* 368: 407–415.
24. Fachi, J. L., J. S. Felipe, L. P. Pral, B. K. da Silva, R. O. Corrêa, M. C. P. de Andrade, D. M. da Fonseca, P. J. Basso, N. O. S. Câmara, É. L. de Sales E Souza, et al. 2019. Butyrate protects mice from *Clostridium difficile*-induced colitis through an HIF-1-dependent mechanism. *Cell Rep.* 27: 750–761.e7.
25. Isa, K., K. Oka, N. Beauchamp, M. Sato, K. Wada, K. Ohtani, S. Nakanishi, E. McCartney, M. Tanaka, T. Shimizu, et al. 2016. Safety assessment of the Clostridium butyricum MIYAIRI 588® probiotic strain including evaluation of antimicrobial sensitivity and presence of Clostridium toxin genes in vitro and teratogenicity in vivo. *Hum. Exp. Toxicol.* 35: 818–832.
26. Takahashi, M., H. Taguchi, H. Yamaguchi, T. Osaki, and S. Kamiya. 2000. Studies of the effect of *Clostridium* butyricum on *Helicobacter pylori* in several test models including gnotobiotic mice. *J. Med. Microbiol.* 49: 635–642.
27. Kuroiwa, T., K. Kobari, and M. Iwanaga. 1990. [Inhibition of enteropathogens by Clostridium butyricum MIYAIRI 588]. *Kansenshogaku Zasshi* 64: 257–263.
28. Woo, T. D. H., K. Oka, M. Takahashi, F. Hojo, T. Osaki, T. Hanawa, S. Kurata, H. Yonezawa, and S. Kamiya. 2011. Inhibition of the cytotoxic effect of *Clostridium difficile* in vitro by *Clostridium* butyricum MIYAIRI 588 strain. *J. Med. Microbiol.* 60: 1617–1625.
29. Hayashi, A., T. Sato, N. Kamada, Y. Mikami, K. Matsuoka, T. Hisamatsu, T. Hibi, A. Roers, H. Yagita, T. Ohteki, et al. 2013. A single strain of *Clostridium* butyricum induces intestinal IL-10-producing macrophages to suppress acute experimental colitis in mice. *Cell Host Microbe* 13: 711–722.
30. Kashiwagi, I., R. Morita, T. Schichita, K. Komai, K. Saeki, M. Matsumoto, K. Takeda, M. Nomura, A. Hayashi, T. Kanai, and A. Yoshimura. 2015. Smad2 and Smad3 inversely regulate TGF-β autoinduction in Clostridium butyricum-activated dendritic cells. *Immunity* 43: 65–79.
31. Takahashi, M., H. Taguchi, H. Yamaguchi, T. Osaki, A. Komatsu, and S. Kamiya. 2004. The effect of probiotic treatment with *Clostridium* butyricum on enterohemorrhagic *Escherichia coli* O157:H7 infection in mice. *FEMS Immunol. Med. Microbiol.* 41: 219–226.
32. Seki, H., M. Shiohara, T. Matsumura, N. Miyagawa, M. Tanaka, A. Komiyama, and S. Kurata. 2003. Prevention of antibiotic-associated diarrhea in children by *Clostridium* butyricum MIYAIRI. *Pediatr. Int.* 45: 86–90.
33. Guinan, J., S. Wang, T. R. Hazbun, H. Yadav, and S. Thangamani. 2019. Antibiotic-induced decreases in the levels of microbial-derived short-chain fatty acids correlate with increased gastrointestinal colonization of *Candida albicans*. *Sci. Rep.* 9: 8872.
34. Tunaru, S., J. Kero, A. Schaub, C. Wufka, A. Blaukat, K. Pfeffer, and S. Offermanns. 2003. PUMA-G and HM74 are receptors for nicotinic acid and mediate its anti-lipolytic effect. *Nat. Med.* 9: 352–355.
35. Tang, C., K. Ahmed, A. Gille, S. Lu, H. J. Gröne, S. Tunaru, and S. Offermanns. 2015. Loss of FFA2 and FFA3 increases insulin secretion and improves glucose tolerance in type 2 diabetes. *Nat. Med.* 21: 173–177.
36. Miyoshi, J., V. Leone, K. Nobutani, M. W. Musch, K. Martinez-Guryn, Y. Wang, S. Miyoshi, A. M. Bobe, A. M. Eren, and E. B. Chang. 2018. Minimizing confounders and increasing data quality in murine models for studies of the gut microbiome. *PeerJ* 6: e5166.
37. Theriot, C. M., M. J. Koenigsknecht, P. E. Carlson, Jr., G. E. Hatton, A. M. Nelson, B. Li, G. B. Huffnagle, J. Z Li, and V. B. Young. 2014. Antibiotic-induced shifts in the mouse gut microbiome and metabolome increase susceptibility to *Clostridium difficile* infection. *Nat. Commun.* 5: 3114.
38. Sato, R., and M. Tanaka. 1997. Intestinal distribution and intraluminal localization of orally administered *Clostridium* butyricum in rats. *Microbiol. Immunol.* 41: 665–671.
39. Hayashi, A., Y. Mikami, K. Miyamoto, N. Kamada, T. Sato, S. Mizuno, M. Naganuma, T. Teratani, R. Aoki, S. Fukuda, et al. 2017. Intestinal dysbiosis and biotin deprivation induce alopecia through overgrowth of *Lactobacillus* murinus in mice. *Cell Rep.* 20: 1513–1524.
40. Caporaso, J. G., K. Bittinger, F. D. Bushman, T. Z. DeSantis, G. L. Andersen, and R. Knight. 2010. PyNAST: a flexible tool for aligning sequences to a template alignment. *Bioinformatics* 26: 266–267.
41. Caporaso, J. G., J. Kuczynski, J. Stombaugh, K. Bittinger, F. D. Bushman, E. K. Costello, N. Fierer, A. G. Peña, J. K. Goodrich, J. I. Gordon, et al. 2010. QIIME allows analysis of high-throughput community sequencing data. *Nat. Methods* 7: 335–336.
42. Edgar, R. C. 2010. Search and clustering orders of magnitude faster than BLAST. *Bioinformatics* 26: 2460–2461.
43. DeSantis, T. Z., P. Hugenholtz, N. Larsen, M. Rojas, E. L. Brodie, K. Keller, T. Huber, D. Dalevi, P. Hu, and G. L. Andersen. 2006. Greengenes, a chimera-checked 16S rRNA gene database and workbench compatible with ARB. *Appl. Environ. Microbiol.* 72: 5069–5072.
44. Wong, J. M., R. de Souza, C. W. Kendall, A. Emam, and D. J. Jenkins. 2006. Colonic health: fermentation and short chain fatty acids. *J. Clin. Gastroenterol.* 40: 235–243.
45. Fournier, B. M., and C. A. Parkos. 2012. The role of neutrophils during intestinal inflammation. *Mucosal Immunol.* 5: 354–366.
46. Witter, A. R., B. M. Okunnu, and R. E. Berg. 2016. The essential role of neutrophils during infection with the intracellular bacterial pathogen *Listeria monocytogenes*. *J. Immunol.* 197: 1557–1565.
47. Selders, G. S., A. E. Fetz, M. Z. Radic, and G. L. Bowlin. 2017. An overview of the role of neutrophils in innate immunity, inflammation and host-biomaterial integration. *Regen. Biomater.* 4: 55–68.
48. Zhang, R., S. Ito, N. Nishio, Z. Cheng, H. Suzuki, and K. Isobe. 2011. Up-regulation of Gr1+CD11b+ population in spleen of dextran sulfate sodium administered mice works to repair colitis. *Inflamm. Allergy Drug Targets* 10: 39–46.
49. Vinolo, M. A., G. J. Ferguson, S. Kulkarni, G. Damoulakis, K. Anderson, M. Bohlooly-Y, L. Stephens, P. T. Hawkins, and R. Curi. 2011. SCFAs induce mouse neutrophil chemotaxis through the GPR43 receptor. *PLoS One* 6: e21205.
50. Hagihara, M., Y. Kuroki, T. Ariyoshi, S. Higashi, K. Fukuda, R. Yamashita, A. Matsumoto, T. Mori, K. Mimura, N. Yamaguchi, et al. 2020. *Clostridium* butyricum modulates the microbiome to protect intestinal barrier function in mice with antibiotic-induced dysbiosis. *iScience* 23: 100772.
51. Gallo, R. L., and L. V. Hooper. 2012. Epithelial antimicrobial defence of the skin and intestine. *Nat. Rev. Immunol.* 12: 503–516.
52. Abt, M. C., B. B. Lewis, S. Caballero, H. Xiong, R. A. Carter, B. Sušac, L. Ling, I. Leiner, and E. G. Pamer. 2015. Innate immune defenses mediated by two ILC subsets are critical for protection against acute *Clostridium difficile* infection. *Cell Host Microbe* 18: 27–37.
53. Okamoto, T., M. Sasaki, T. Tsujikawa, Y. Fujiyama, T. Bamba, and M. Kusunoki. 2000. Preventive efficacy of butyrate enemas and oral administration of *Clostridium* butyricum M588 in dextran sodium sulfate-induced colitis in rats. *J. Gastroenterol.* 35: 341–346.
54. Park, J., M. Kim, S. G. Kang, A. H. Jannasch, B. Cooper, J. Patterson, and C. H. Kim. 2015. Short-chain fatty acids induce both effector and regulatory T cells by suppression of histone deacetylases and regulation of the mTOR-S6K pathway. *Mucosal Immunol.* 8: 80–93.
55. Kitamoto, S., C. J. Alteri, M. Rodrigues, H. Nagao-Kitamoto, K. Sugihara, S. D. Himpsl, M. Bazzi, M. Miyoshi, T. Nishioka, A. Hayashi, et al. 2020. Dietary L-serine confers a competitive fitness advantage to Enterobacteriaceae in the inflamed gut. *Nat. Microbiol.* 5: 116–125.
56. Etienne-Mesmin, L., B. Chassaing, O. Adekunle, L. M. Mattei, F. D. Bushman, and A. T. Gewirtz. 2018. Toxin-positive *Clostridium difficile* latently infect mouse colonies and protect against highly pathogenic *C. difficile*. *Gut* 67: 860–871.